An enhancement of the warping shear functions of Refined Zigzag Theory

An enhancement of the warping shear functions of Refined Zigzag Theory

M. Sorrenti[(1)*], M. Di Sciuva[(2)]

[(1)] Department of Mechanical and Aerospace Engineering – Politecnico di Torino, Corso Duca degli Abruzzi 24, 10129 Torino, Italy, matteo.sorrenti@polito.it

[(2)] Former Professor of Aircraft Structures at Department of Mechanical and Aerospace Engineering – Politecnico di Torino, Corso Duca degli Abruzzi 24, 10129 Torino, Italy, marco.disciuva@formerfaculty.polito.it

Abstract

The paper presents an enhancement in Refined Zigzag Theory (RZT) for the analysis of multilayered composite plates. In standard RZT, the zigzag functions cannot predict the coupling effect of in-plane displacements for anisotropic multilayered plates, such as angle-ply laminates. From a computational point of view, this undesirable effect leads to a singular stiffness matrix. In this work, the local kinematic field of RZT is enhanced with the other two zigzag functions that allow the coupling effect. In order to assess the accuracy of these new zigzag functions for RZT, results obtained from bending of angle-ply laminated plates are compared to the three-dimensional exact elasticity solutions and other plate models used in the open literature. The numerical results highlight that the enhanced zigzag functions extend the range of applicability of RZT to the study of general angle-ply multilayered structures, maintaining the same seven kinematic unknowns of standard RZT.

Keywords: Refined Zigzag Theory; angle-ply multilayered plates; warping shear functions.

https://doi.org/10.1115/1.4050908

* Corresponding Author: Matteo Sorrenti, email: matteo.sorrenti@polito.it Tel. +39 3337120343.

1. Introduction

In the last decades, multilayered composite and sandwich structures have been increasingly used in aerospace, marine, military, civil, and automotive industries due to their excellent high specific strength and stiffness, good fatigue behavior, and damping characteristics. On the other hand, their transverse shear deformability and through-the-thickness anisotropy demand for accurate computational models to reliably predict their structural response at affordable computational costs.

In order to obtain a solution for the largest number of structural plate problems, the axiomatic displacement-based theories are widely considered. Such models can be divided into two macro-areas: the Equivalent Single Layer (ESL) theories and the Layer-Wise (LW) theories. The interested reader is referred, among the others, to Refs. [1,2]. Simply stated, the former assumes a through-the-thickness distribution of the displacement field along with the entire laminate thickness. In the latter, the displacement field is assumed independent for each layer, and it is possible to ensure the continuity of transverse stresses at the interfaces (a condition that cannot be obtained directly in ESL theories). Among the ESL theories, the Classical Laminate Theory (CLT), the First Order Shear deformation Theory (FSDT), the Reddy's Third Order Shear deformation Theory (TSDT) should be cited. Depending on the plate aspect ratio, these theories are more or less accurate to predict general quantities such as transverse displacements, fundamental frequencies, buckling loads, but generally are not accurate to predict local quantities (in-plane displacements, strain and stresses distributions). On the other hand, LW theories accurately predict the previous global and local quantities, but the computational cost becomes prohibitive for plates with several layers.

The Zig-Zag Theories represent a good compromise between the reduced number of unknown variables of ESL and the good accuracy LW theories. In such models, the kinematic field is a superposition of a coarse and a finer distribution of in-plane displacement. The accuracy of displacements and in-plane stresses are improved by the zigzag functions, typically piecewise linear. This enhancement leads to having a fixed number of unknown variables while maintaining a good accuracy in thickness-wise distributions of in-plane displacements and stresses typically of a multilayered plate. Many researchers have put their efforts in this field, typically starting from an assumed shear stress field, among which Whitney [3] is worth mentioning. Other significative works are those represented by Murakami [4], Di Sciuva [5] and Cho and Parmerter [6], who assumed a zigzag contribution directly superimposed in the kinematic field to study general laminates. Moreover, recently Loredo and co-workers [7,8], formulated a family of improved theories with a set of transverse shear warping functions to study the behaviour of general laminates. It is worthy to note that such functions are very accurate since they satisfy exactly the C_z^0 requirements. On the other hand, if the form of warping shear

functions is assumed *a-priori* in the kinematic field, the continuity of displacements and transverse shear stresses have to be enforced *a-posteriori* at layer interfaces.

Recently, Tessler and co-workers formulated an accurate refined theory, here named standard Refined Zigzag Theory (RZT), for the analysis of multilayered composite and sandwich structures [9]. In Tessler et al. [10], it has been shown that standard RZT is also capable of investigating, with an appropriate methodology, the behaviour of homogeneous plates. Gherlone [11] deeply investigated the role of zigzag functions in the ESL refinement to analyse multilayered composite and sandwich beams. Iurlaro et al. [12] have improved the linear RZT model with cubic zigzag function to analyse thick multilayered beams. An interesting aspect is that standard RZT requires only C^0 continuity in finite element formulation, and this makes this theory very attractive from a computational point of view.

Recently, Kreja and Sabik [13] have compared some zigzag models to analyse laminated multilayered plates, highlighting a drawback of standard RZT. Due to the kinematic field's assumptions in standard RZT, it is impossible to study multilayered angle-ply plates in which two adjacent laminae have alternating orientations, but the same absolute value. In such cases, the slope of zigzag functions is constant for each layer and, in order to satisfy the null value for these functions at the external surfaces, it results that they are constant and null through-the-thickness. Thus, the local displacement field is null, although it has been considered a multilayered structures, and from a computational point of view, this leads to a singular stiffness matrix. No other investigations on angle-ply or general laminated plate using standard RZT are present in literature.

Following the generalization of Di Sciuva's zigzag model [14] and taking into account the drawback of standard RZT to study angle-ply laminates, the purpose of this work is to enhance the standard Refined Zigzag Theory in order to allow the analysis of more general anisotropic multilayered laminates and sandwich plates.

2. Enhanced Refined Zigzag Theory

2.1 Geometrical preliminaries

We consider a multilayered flat rectangular plate made of a finite number N of perfectly bonded layers. V is the volume of the plate, h the thickness; a_1 and a_2 are the length and width, respectively. The points of the plate are referred to an orthogonal Cartesian coordinate system defined by the vector $\mathbf{X}=\{x_i\}$ $(i=1,2,3)$. The vector $\mathbf{x}=\{x_\alpha\}$ $(\alpha=1,2)$ represents the set of in-plane coordinates on the reference plane Ω, here chosen to be the middle plane of the plate, and x_3 being the coordinate normal to the reference plane, so that x_3 is defined in the range $x_3 \in \left[-\frac{h}{2},+\frac{h}{2}\right]$. The origin of the reference frame is fixed so $x_1 \in [0,+a_1]$ and $x_2 \in [0,+a_2]$. The thickness of each layer, as well as of the whole plate,

is assumed to be constant, and the material of each layer is assumed to be elastic orthotropic with a plane of elastic symmetry parallel to the reference surface and whose principal orthotropy directions are arbitrarily oriented with respect to the in-plane reference frame.

If not otherwise stated in the paper, the superscript (k) is used to indicate quantities corresponding to the k^{th} layer (k=1,…,N), whereas the notation $(.)_{(k)}$ (k=1,…,N-1) stands for (.) valued for $x_3 = z_{(k)}$, i.e., at the k^{th} interface (k=1,…,N-1) between the k^{th} and the $(k+1)^{\text{th}}$ layer. Also, we use the subscript (B) and (T) to indicate the bottom and top surfaces, respectively, of the single-layer/whole plate; specifically, $z_{(\text{B})}^{(1)} = z_{(\text{B})}$ and $z_{(\text{T})}^{(N)} = z_{(\text{T})}$ denote the coordinates of the bottom and top surfaces of the whole plate; thus, $h = z_{(\text{T})} - z_{(\text{B})} = z_{(N)} - z_{(0)}$ is the plate thickness and $h^{(k)} = z_{(k)} - z_{(k-1)} = z_{(\text{T})}^{(k)} - z_{(\text{B})}^{(k)}$ $(k = 1,2,...,N)$, the thickness of the k^{th} layer.

The symbol $(\bullet)_{,i} = \dfrac{\partial(\bullet)}{\partial x_i}$ refers to the derivative of the function $(\bullet)$ with respect to the coordinate x_i, i.e., $(\bullet)_{,i} = \dfrac{\partial(\bullet)}{\partial x_i}$.

In the paper, if not otherwise specified, the Einsteinian summation convention over repeated indices is adopted, with Latin indices ranging from 1 to 3, and Greek indices ranging from 1 to 2.

2.2 Kinematics

As usual in the axiomatic theories of plates and shells, the thickness-wise distribution of the 3-D displacement field is assumed *a-priori*. Specifically, in the enhanced RZT, following the standard RZT, the in-plane kinematics is based on the superposition of a global (G) first-order kinematics (which is continuous with its first derivatives with respect to the x_3-coordinate) and a local (L) layer-wise correction of the in-plane displacements (which is continuous and piecewise linear with respect to x_3, but with jumps in the first derivative at the interface between adjacent layers), while the transverse deflection is assumed to be uniform along with the thickness. Thus,

$$\tilde{\mathbf{u}}^{(k)}(\mathbf{X}) = \tilde{\mathbf{u}}^{G}(\mathbf{X}) + \tilde{\mathbf{u}}^{L}(\mathbf{X}); \quad \tilde{u}_3^{(k)}(\mathbf{X}) = u_3(\mathbf{x}) \tag{1}$$

where

$$\tilde{\mathbf{u}}^{G}(\mathbf{X}) = \mathbf{u}(\mathbf{x}) + x_3\boldsymbol{\theta}(\mathbf{x}); \;\; \tilde{\mathbf{u}}^{L(k)}(\mathbf{X}) = \boldsymbol{\phi}^{(k)}(x_3)\boldsymbol{\psi}(\mathbf{x}) \tag{2}$$

$$\tilde{\mathbf{u}}^{(k)}(\mathbf{X}) = \begin{Bmatrix} \tilde{u}_1(\mathbf{X}) \\ \tilde{u}_2(\mathbf{X}) \end{Bmatrix}^{(k)}; \; \mathbf{u}(\mathbf{x}) = \begin{Bmatrix} u_1(\mathbf{x}) \\ u_2(\mathbf{x}) \end{Bmatrix}; \; \boldsymbol{\theta}(\mathbf{x}) = \begin{Bmatrix} \theta_1(\mathbf{x}) \\ \theta_2(\mathbf{x}) \end{Bmatrix} \tag{3}$$

$$\boldsymbol{\phi}^{(k)}(x_3) = \begin{bmatrix} \phi_{11}^{(k)}(x_3) & \phi_{12}^{(k)}(x_3) \\ \phi_{21}^{(k)}(x_3) & \phi_{22}^{(k)}(x_3) \end{bmatrix}; \; \boldsymbol{\psi}(\mathbf{x}) = \begin{Bmatrix} \psi_1(\mathbf{x}) \\ \psi_2(\mathbf{x}) \end{Bmatrix} \tag{4}$$

In Eq. (2), $\mathbf{u}(\mathbf{x})$ and $\boldsymbol{\theta}(\mathbf{x})$ are the global in-plane displacements and rotations of the normal to the reference plane about the positive x_2 and the negative x_1 directions, respectively; $\boldsymbol{\psi}(\mathbf{x})$ denotes the matrix of the unknown spatial amplitudes of the $\boldsymbol{\phi}^{(k)}(x_3)$ zigzag functions, these last being assumed piecewise linear functions through-the-thickness, vanishing on the top and bottom surfaces of the plate[1]. Moreover, $u_3(\mathbf{x})$ is the transverse deflection, assumed to be constant along with the plate thickness.

2.3 Stress-strain relations

As usual in plate theory, a plane stress state is assumed, i.e., $\tilde{\sigma}_{33} = 0$. According to this assumption, the reduced local elastic Hookean constitutive equations read

$$\tilde{\boldsymbol{\sigma}}_p^{(k)} = \bar{\mathbf{Q}}_p^{(k)} \tilde{\boldsymbol{\varepsilon}}_p^{(k)}; \;\; \tilde{\boldsymbol{\sigma}}_t^{(k)} = \bar{\mathbf{Q}}_t^{(k)} \boldsymbol{\gamma}_t^{(k)} \tag{5}$$

In Eq. (5),

$$\tilde{\boldsymbol{\sigma}}_{\mathrm{p}}^{(k)T} = \begin{bmatrix} \tilde{\sigma}_{11} & \tilde{\sigma}_{22} & \tilde{\sigma}_{12} \end{bmatrix}^{(k)}, \quad \tilde{\boldsymbol{\sigma}}_{\mathrm{t}}^{(k)} = \begin{bmatrix} \tilde{\sigma}_{13} & \tilde{\sigma}_{23} \end{bmatrix}^{(k)T} \tag{6}$$

are the in-plane and transverse shear stresses, respectively;

$$\tilde{\boldsymbol{\varepsilon}}_{\mathrm{p}}^{(k)T} = \begin{bmatrix} \tilde{\varepsilon}_{11} & \tilde{\varepsilon}_{22} & \tilde{\gamma}_{12} = 2\tilde{\varepsilon}_{12} \end{bmatrix}^{(k)T}; \;\; \boldsymbol{\gamma}_{\mathrm{t}}^{(k)T} = \begin{bmatrix} \tilde{\gamma}_{13} & \tilde{\gamma}_{23} \end{bmatrix}^{(k)T} \tag{7}$$

are the in-plane and transverse shear strains, and

$$\bar{\mathbf{Q}}_{\mathrm{p}}^{(k)} = \begin{bmatrix} \bar{Q}_{11} & \bar{Q}_{12} & \bar{Q}_{16} \\ \bar{Q}_{12} & \bar{Q}_{22} & \bar{Q}_{26} \\ \bar{Q}_{16} & \bar{Q}_{26} & \bar{Q}_{66} \end{bmatrix}^{(k)}, \quad \bar{\mathbf{Q}}_{\mathrm{t}}^{(k)} = \begin{bmatrix} \bar{Q}_{44} & \bar{Q}_{45} \\ \bar{Q}_{45} & \bar{Q}_{55} \end{bmatrix}^{(k)} \tag{8}$$

In Eq.(8), $\bar{Q}_{ij}^{(k)}$ (i,j=1,2,6) denote the transformed plane stress elastic reduced stiffness coefficients; $\bar{Q}_{ij}^{(k)}$ (i,j=4,5) denote the transformed transverse shear elastic stiffness coefficients.

Using the linear strain-displacement relations and by taking into account the assumed kinematics, we obtain

$$\tilde{\boldsymbol{\varepsilon}}_{\mathrm{p}}^{(k)} = \boldsymbol{\varepsilon}^{(\mathrm{m})} + x_3 \boldsymbol{\varepsilon}^{(\mathrm{b})} + \boldsymbol{\Phi}^{(k)}(x_3) \boldsymbol{\varepsilon}^{(\phi)}; \qquad \tilde{\boldsymbol{\gamma}}_t^{(k)} = \boldsymbol{\gamma}^{(0)} + \boldsymbol{\phi}_{,3}^{(k)} \boldsymbol{\psi} = \boldsymbol{\gamma}^{(0)} + \boldsymbol{\beta}^{(k)} \boldsymbol{\psi} \tag{9}$$

where

$$\boldsymbol{\varepsilon}^{(\mathrm{m})T} = \begin{bmatrix} u_{1,1} & u_{2,2} & u_{1,2} + u_{2,1} \end{bmatrix}, \;\; \boldsymbol{\varepsilon}^{(\mathrm{b})T} = \begin{bmatrix} \theta_{1,1} & \theta_{2,2} & \theta_{1,2} + \theta_{2,1} \end{bmatrix} \tag{10}$$

$$\boldsymbol{\varepsilon}^{(\phi)} = \begin{Bmatrix} \psi_{1,1} \\ \psi_{2,2} \\ \psi_{1,2} \\ \psi_{2,1} \end{Bmatrix}, \;\; \boldsymbol{\Phi}^{(k)}(x_3) = \begin{bmatrix} \phi_{11}^{(k)} & 0 & 0 & \phi_{12}^{(k)} \\ 0 & \phi_{22}^{(k)} & \phi_{21}^{(k)} & 0 \\ \phi_{21}^{(k)} & \phi_{12}^{(k)} & \phi_{11}^{(k)} & \phi_{22}^{(k)} \end{bmatrix} \tag{11}$$

$$\boldsymbol{\gamma}^{(0)} = \begin{Bmatrix} \gamma_1^{(0)} \\ \gamma_2^{(0)} \end{Bmatrix} = \begin{Bmatrix} \theta_1 + u_{3,1} \\ \theta_2 + u_{3,2} \end{Bmatrix} = \boldsymbol{\theta} + \boldsymbol{\Delta} u_3, \;\; \boldsymbol{\beta}^{(k)} = \boldsymbol{\phi}_{,3}^{(k)} \tag{12}$$

[1] Note that, contrary to standard RZT, $\boldsymbol{\phi}^{(k)}(x_3)$ now is not diagonal, due to the off-diagonal (coupling) terms.

Note that in the general case of a multilayered plate the through-the-thickness distribution of the transverse shear stresses are piecewise-constant with jumps at the interfaces.

2.4 Derivation of the enhanced zigzag functions

The enhanced zigzag functions' derivation follows the same path as that adopted in standard RZT [9,11]. So, for the sake of brevity, the intermediate passages are not shown here. We introduce the auxiliary strain measure vector,

$$\boldsymbol{\eta}(\mathbf{x}) = \boldsymbol{\gamma}^{(0)}(\mathbf{x}) - \boldsymbol{\psi}(\mathbf{x}) \tag{13}$$

and rewrite the transverse shear stresses as follows

$$\tilde{\boldsymbol{\sigma}}_{\mathrm{t}}^{(k)} = \tilde{\boldsymbol{\sigma}}_{\mathrm{t}}^{\mathrm{d}(k)} + \tilde{\boldsymbol{\sigma}}_{\mathrm{t}}^{\mathrm{c}(k)} \tag{14}$$

with (**I** stands for the identity matrix)

$$\tilde{\boldsymbol{\sigma}}_{\mathrm{t}}^{\mathrm{d}(k)} = \bar{\mathbf{Q}}_{\mathrm{t}}^{(k)} \boldsymbol{\eta}(\mathbf{x}); \quad \tilde{\boldsymbol{\sigma}}_{\mathrm{t}}^{\mathrm{c}(k)} = \bar{\mathbf{Q}}_{\mathrm{t}}^{(k)} \left(\mathbf{I} + \boldsymbol{\beta}^{(k)} \right) \boldsymbol{\psi} \tag{15}$$

Enforcing the continuity conditions on $\tilde{\boldsymbol{\sigma}}_{\mathrm{t}}^{\mathrm{c}(k)}$ at the interface k, i.e., $\tilde{\boldsymbol{\sigma}}_{\mathrm{t}}^{\mathrm{c}(k)} \left(z_{(\mathrm{T})}^{(k)} \right) = \tilde{\boldsymbol{\sigma}}_{\mathrm{t}}^{\mathrm{c}(k+1)} \left(z_{(\mathrm{B})}^{(k+1)} \right)$, and remembering that within each layer, $\bar{\mathbf{Q}}_{\mathrm{t}}^{(k)} \left(\mathbf{I} + \boldsymbol{\beta}^{(k)} \right) \boldsymbol{\psi}$ is constant, yields

$$\bar{\mathbf{Q}}_{\mathrm{t}}^{(k)} \left(\mathbf{I} + \boldsymbol{\beta}^{(k)} \right) \boldsymbol{\psi} = \bar{\mathbf{Q}}_{\mathrm{t}}^{(k+1)} \left(\mathbf{I} + \boldsymbol{\beta}^{(k+1)} \right) \boldsymbol{\psi} = \mathbf{G} \boldsymbol{\psi} \tag{16}$$

where **G** is a (2x2) matrix whose entries are independent of the layer; they are *zigzag weighted-average transverse shear moduli of the whole plate*. Solving Eq. (16) for $\boldsymbol{\beta}^{(k)}$ yields the expression for the thickness-wise derivative of the zigzag function in the enhanced RZT,

$$\boldsymbol{\beta}^{(k)} = \mathbf{Q}_{\mathrm{t}}^{(k)^{-1}} \mathbf{G} - \mathbf{I} = \mathbf{S}_{\mathrm{t}}^{(k)} \mathbf{G} - \mathbf{I} \tag{17}$$

where $\mathbf{S}_{\mathrm{t}}^{(k)} = \mathbf{Q}_{\mathrm{t}}^{(k)^{-1}}$ is the (2x2) symmetric matrix of the transverse shear compliance coefficients of the k^{th} layer. Integrating Eq. (17) over the thickness and by enforcing the condition that the local contribution is zero on the top and bottom surfaces of the whole plate**,** yields

$$\mathbf{G} = (z_{(\mathrm{T})} - z_{(\mathrm{B})}) \left(\sum_{k=1}^{N} (z_{(\mathrm{T})}^{(k)} - z_{(\mathrm{B})}^{(k)}) \mathbf{S}_{\mathrm{t}}^{(k)} \right)^{-1} = h \left(\sum_{k=1}^{N} h^{(k)} \mathbf{S}_{\mathrm{t}}^{(k)} \right)^{-1} \tag{18}$$

Substituting Eq. (18) into Eq. (17) and integrating over the thickness, yields

$$\boldsymbol{\phi}^{(k)}(x_3) - \boldsymbol{\phi}^{(k)}(z_{(\mathrm{B})}^{(k)}) = (x_3 - z_{(\mathrm{B})}^{(k)}) \left(\mathbf{S}_{\mathrm{t}}^{(k)} \mathbf{G} - \mathbf{I} \right) \quad (z_{(\mathrm{B})}^{(k)} \le x_3 \le z_{(\mathrm{T})}^{(k)}) \tag{19}$$

with

$$z_{(\mathrm{B})}^{(k)} = z_{(\mathrm{B})} + \sum_{q=1}^{k-1} (z_{(\mathrm{T})}^{(q)} - z_{(\mathrm{B})}^{(q)}) = z_{(\mathrm{B})} + \sum_{q=1}^{k-1} h^{(q)} \quad k = 2,3,...,N \tag{20}$$

It is easy to show that Eq. (19) can be cast in the following recursive formula

$$\begin{aligned}\boldsymbol{\phi}^{(k)}(x_3) &= (x_3 - z_{(\mathrm{B})})\left(\mathbf{S}_{\mathrm{t}}^{(k)}\mathbf{G} - \mathbf{I}\right) + \sum_{q=1}^{k} h^{(q)}\left(\mathbf{S}_{\mathrm{t}}^{(q)} - \mathbf{S}_{\mathrm{t}}^{(k)}\right)\mathbf{G} \\ &= (x_3 - z_{(\mathrm{B})})\boldsymbol{\beta}^{(k)} + \sum_{q=1}^{k} h^{(q)}\left(\boldsymbol{\beta}^{(q)} - \boldsymbol{\beta}^{(k)}\right) \qquad (k = 1,...,N)\end{aligned} \tag{21}$$

At this point, the expression for $\boldsymbol{\beta}^{(k)}$ matrix, as given by Eq. (17), can be used in Eq. (9) to obtain the through-the-thickness transverse shear strain distributions, i.e. $\boldsymbol{\gamma}_t^{(k)}$. This allows to compute the transverse shear stresses using Eq. (5) and Eq. (9) in terms of the kinematic unknowns.

2.5 Equilibrium equations and boundary conditions

The principle of virtual work is used herein to derive the equilibrium equations and the variationally consistent boundary conditions. The principle can be stated as follows (here δ stands for the variational operator)

$$\delta W_{\mathrm{int}} - \delta W_{\mathrm{ex}} = 0 \tag{22}$$

where

$$\delta W_{\mathrm{int}} = \int_{\Omega} \left\langle \tilde{\boldsymbol{\sigma}}^{(k)T} \delta \tilde{\boldsymbol{\varepsilon}}^{(k)} \right\rangle d\Omega \tag{23}$$

is the virtual variation of the internal work given by the stresses $\tilde{\boldsymbol{\sigma}}^{(k)}$, and

$$\delta W_{\mathrm{ex}} = \int_{\Omega} \bar{p}_3 \delta u_3^{(0)} d\Omega \tag{24}$$

is the virtual variation of the work done by the applied loads. It is assumed that only the transverse load $\bar{p}_3$ is acting on the plate. Moreover, $\left\langle \bullet \right\rangle = \sum_{k=1}^{N} \int_{x_3^{(k-1)}}^{x_3^{(k)}} (\bullet) dx_3 = \sum_{k=1}^{N} \int_{z_{(\mathrm{B})}^{(k)}}^{z_{(\mathrm{T})}^{(k)}} (\bullet) dx_3$. Substitution of Eq. (5) into Eq. (23), yields

$$\boldsymbol{\delta} W_{\mathrm{int}} = \int_{\Omega} \left(\mathbf{R}_{\mathrm{p}}^{T} \delta \boldsymbol{\varepsilon}_{\mathrm{p}} + \mathbf{R}_{\mathrm{t}}^{T} \delta \boldsymbol{\gamma} \right) d\Omega \tag{25}$$

where

$$\mathbf{R}_{\mathrm{p}}^{T} = \begin{bmatrix} \mathbf{N}^{T} & \mathbf{M}^{T} & \mathbf{M}^{(\phi)T} \end{bmatrix}; \;\; \mathbf{R}_{\mathrm{t}}^{T} = \begin{bmatrix} \mathbf{T}^{T} & \mathbf{T}^{(\phi)T} \end{bmatrix} \tag{26}$$

In Eq. (26) the following force and moment stress resultants for unit length have been introduced

$$\left(\mathbf{N}, \mathbf{M}, \mathbf{M}^{(\phi)}\right) = \left(\begin{Bmatrix} N_{11} \\ N_{22} \\ N_{12} \end{Bmatrix}, \begin{Bmatrix} M_{11} \\ M_{22} \\ M_{12} \end{Bmatrix}, \begin{Bmatrix} M_{11}^{(\phi)} \\ M_{22}^{(\phi)} \\ M_{12}^{(\phi)} \\ M_{21}^{(\phi)} \end{Bmatrix} \right) = \left\langle \left(1, x_3, \boldsymbol{\Phi}^{(k)\mathrm{T}}\right) \tilde{\boldsymbol{\sigma}}_{\mathrm{p}}^{(k)} \right\rangle \tag{27}$$

$$\left(\mathbf{T}, \mathbf{T}^{(\phi)}\right) = \left(\begin{Bmatrix} T_1 \\ T_2 \end{Bmatrix}, \begin{Bmatrix} T_1^{(\phi)} \\ T_2^{(\phi)} \end{Bmatrix} \right) = \left\langle \left(1, \boldsymbol{\phi}_{,3}^{(k)}\right) \tilde{\boldsymbol{\sigma}}_{t}^{(k)} \right\rangle \tag{28}$$

The plate constitutive relations of enhanced RZT are derived by using Eq. (5) into the Eqs. (27)-(28), and integrating over the plate thickness. It results in

$$\left\{\begin{array}{c}\mathbf{N}\\ \mathbf{M}\\ \mathbf{M}^{(\phi)}\end{array}\right\}=\left[\begin{array}{ccc}\mathbf{A} & \mathbf{B} & \mathbf{A}^{(\phi)}\\ \mathbf{B} & \mathbf{D} & \mathbf{B}^{(\phi)}\\ \mathbf{A}^{(\phi)T} & \mathbf{B}^{(\phi)T} & \mathbf{D}^{(\phi)}\end{array}\right]\left\{\begin{array}{c}\boldsymbol{\varepsilon}^{(\mathrm{m})}\\ \boldsymbol{\varepsilon}^{(\mathrm{b})}\\ \boldsymbol{\varepsilon}^{(\phi)}\end{array}\right\};\quad \left\{\begin{array}{c}\mathbf{T}\\ \mathbf{T}^{(\phi)}\end{array}\right\}=\left[\begin{array}{cc}\mathbf{A}_{\mathrm{t}} & \mathbf{B}_{\mathrm{t}}^{(\phi)}\\ \mathbf{B}_{\mathrm{t}}^{(\phi)T} & \mathbf{D}_{\mathrm{t}}^{(\phi)}\end{array}\right]\left\{\begin{array}{c}\boldsymbol{\gamma}^{(0)}\\ \boldsymbol{\psi}\end{array}\right\} \tag{29}$$

where

$$\begin{aligned}&\left(\mathbf{A},\mathbf{B},\mathbf{D}\right)=\left\langle\bar{\mathbf{Q}}_{\mathrm{p}}^{(k)}(1,x_3,x_3^2)\right\rangle,\ \left(\mathbf{A}^{(\phi)},\mathbf{B}^{(\phi)},\mathbf{D}^{(\phi)}\right)=\left\langle\left(1,x_3,\boldsymbol{\Phi}^{(k)\mathrm{T}}\right)\bar{\mathbf{Q}}_{\mathrm{p}}^{(k)}\boldsymbol{\Phi}^{(k)}\right\rangle\\ &\left(\mathbf{A}_{\mathrm{t}},\mathbf{B}_{\mathrm{t}}^{(\phi)}\right)=\left\langle\bar{\mathbf{Q}}_{\mathrm{t}}^{(k)}\left(1,\boldsymbol{\phi}_{,3}^{(k)}\right)\right\rangle,\quad \mathbf{D}_{\mathrm{t}}^{(\phi)}=\left\langle\boldsymbol{\phi}_{,3}^{(k)\mathrm{T}}\bar{\mathbf{Q}}_{\mathrm{t}}\boldsymbol{\phi}_{,3}^{(k)}\right\rangle\end{aligned} \tag{30}$$

Substituting Eqs.(9), (24) and (25) into the principle of virtual work (Eq. (22)), after a tedious, but straightforward, integration by parts, rearranging the various contributions and setting equal to zero the coefficients of the virtual variations of the generalized coordinates in domain and boundary integrals, yields the following variationally consistent equilibrium equations in terms of the stress resultants ($\mathbf{R}_{\mathrm{p}}$, $\mathbf{R}_{\mathrm{t}}$):

$$\begin{aligned}&\delta u_\alpha)\quad N_{\alpha\beta,\beta}=0\,;\quad \delta\theta_\alpha)\quad M_{\alpha\beta,\beta}-T_\alpha=0\\ &\delta u_3)\quad T_{\mu,\mu}=-\bar{p}_3\,;\quad \delta\psi_\alpha)\quad M_{\alpha\beta,\beta}^{(\phi)}-T_\alpha^{(\phi)}=0\end{aligned} \tag{31}$$

along with the variationally consistent boundary conditions. With reference to a rectangular plate of dimensions a_1 and a_2 along the edges parallel to the x_1 and x_2-axes, here below, we have listed the boundary conditions (BCs) used in the numerical analysis:

Anti-symmetric angle-ply simply supported on all edges, read

$$@\ x_1=0,a_1\text{:}\qquad u_1=u_3=N_{12}=M_{11}=M_{11}^{(\phi)}=0$$

$$@\ x_2=0,a_2\text{:}\qquad u_2=u_3=N_{12}=M_{22}=M_{22}^{(\phi)}=0$$

Symmetric angle-ply simply supported on two opposite edges and infinite length in x_2 direction, read

$$@\ x_1=0,a_1\text{:}\qquad u_3=N_{11}=N_{12}=M_{11}=M_{12}=M_{11}^{(\phi)}=M_{12}^{(\phi)}=0$$

Using the constitutive relations (i.e. Eqs. (29)), both the equilibrium equations and the boundary conditions can be given in terms of the generalized displacements. For the sake of brevity, they are not given here.

3. Numerical Analysis

In order to assess the accuracy of enhanced RZT with the new set of zigzag functions (en-RZT), some numerical tests have been carried out. The numerical investigation has been performed on general laminated plates for which the three-dimensional solutions are available in the open literature. The results from 3D solutions obtained using analytic approaches are labelled in the following part of the paper as "*3D*". The equilibrium equations and consistent boundary conditions of the en-RZT model, for the numerical examples here investigated, are solved using the Navier-type solution with the appropriate trigonometric expansions [9]. The following material properties are assumed for each layer:

$$E_L / E_T = 25 \quad G_{LT} / E_T = 0.5 \quad G_{TT} / E_T = 0.2 \quad \nu_{LT} = \nu_{TT} = 0.25$$

where *L* and *T* are longitudinal and transverse directions of the fibres, respectively.

In the first numerical example, an antisymmetric two-layered angle-ply ($a_1/a_2=1$) laminate (L1) is considered. Each layer has the same thickness, and it is simply supported on all the edges and subjected to a bi-sinusoidal transverse pressure. In the second numerical example, a symmetric three-layered angle-ply laminate (L2) is considered under cylindrical bending conditions and simply supported boundary conditions. The laminate L2 has ply thickness (0.25/0.5/0.25) and lamina orientations (30°/-30°/30°).

3.1 Enhanced zigzag functions

A brief comparison between standard and enhanced zigzag functions has been made for the angle-ply laminate L1. In Figure 1, the corresponding four zigzag functions are displayed for the angle-ply laminate with (-15°/15°) lamination angles. Clearly, in standard RZT, the zigzag functions ϕ_{12} and ϕ_{21} are not considered since there is no coupling effect. In the enhanced model, ϕ_{11} and ϕ_{22} are still not present for this type of lamination scheme, but the model is now capable of predicting the zigzag coupling functions ϕ_{12} and ϕ_{21}. It can be noted, for cross-ply laminated and sandwich plates, the standard zigzag functions are fully recovered using this model. Another important aspect of this improved model is to have solved the problem of singularity due to zero zigzag functions, typical of the classical one.

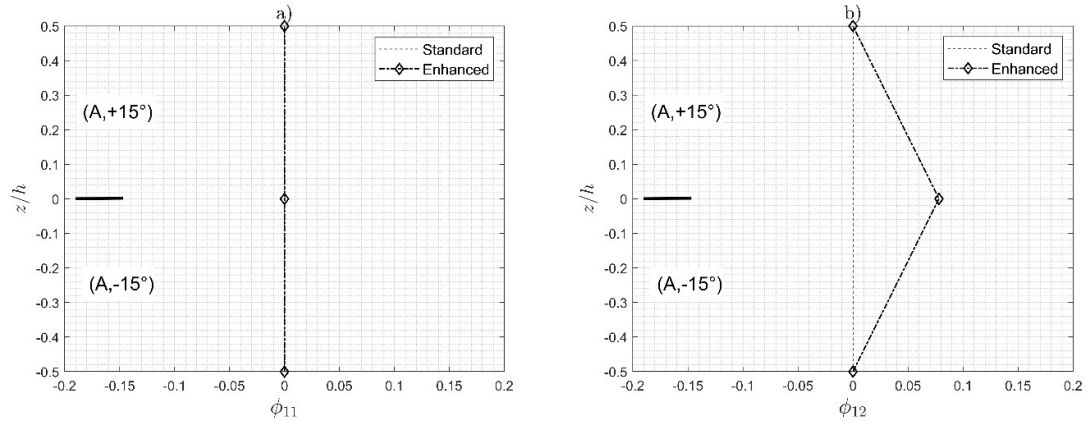

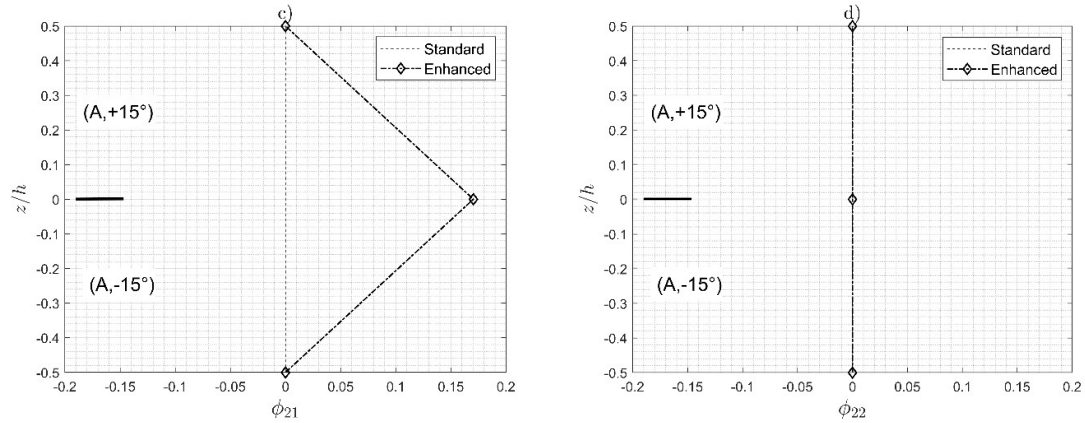

Figure 1 - Zigzag functions for standard and enhanced RZT, anti-symmetric angle-ply (L1).

3.2 Static analysis

Problem 1 – Simply supported plates under bi-sinusoidal transverse load

In this section, a static analysis of general composite laminated plates is made to assess the computational improvements of en-RZT. Since, for a cross-ply multilayered plate, the present procedure yields the same zigzag functions of standard RZT, we focus the attention on the analysis of anisotropic plates, such as angle-ply plates.

In this first numerical assessment, we consider the two-layered angle-ply (*-θ/θ*) plate (L1), simply supported and subjected to a bi-sinusoidal transverse pressure $\bar{p}_3(x_1,x_2)=\bar{p}_0\sin\left(\pi\frac{x_1}{a_1}\right)\cos\left(\pi\frac{x_2}{a_2}\right)$, with various lamination angle. For this case, the exact 3D solution is available in literature, Ref. [15]. The trigonometric expansions that satisfy the equilibrium equations and the simply supported boundary conditions are:

$$u_1=U_1\sin\left(\pi x_1/a_1\right)\cos\left(\pi x_2/a_2\right);\qquad u_2=U_2\cos\left(\pi x_1/a_1\right)\sin\left(\pi x_2/a_2\right);$$
$$u_3=U_3\sin\left(\pi x_1/a_1\right)\sin\left(\pi x_2/a_2\right);$$
$$\begin{Bmatrix}\theta_1\\ \psi_1\end{Bmatrix}=\begin{Bmatrix}\Theta_1\\ \Psi_1\end{Bmatrix}\cos\left(\pi x_1/a_1\right)\sin\left(\pi x_2/a_2\right);\qquad \begin{Bmatrix}\theta_2\\ \psi_2\end{Bmatrix}=\begin{Bmatrix}\Theta_2\\ \Psi_2\end{Bmatrix}\sin\left(\pi x_1/a_1\right)\cos\left(\pi x_2/a_2\right)$$

Table 1 – Non-dimensional maximum deflections $\left(100u_3\,E_T h^3/\bar{p}_0 a_1^4\right)$ of simply supported two-layered angle-ply plates (L1) under bi-sinusoidal transverse pressure

	a1/h=4 - a1/a2=1		*a1/h=10 - a1/a2=1*		*a1/h=4 - a1/a2=1/3*	
θ [°]	3D [15]	Present	3D [15]	Present	3D [15]	Present
15	1.7059	1.6054	0.8027	0.7821	2.4903	2.3578
30	1.7297	1.6358	0.8568	0.8388	3.4118	3.2606
45	1.6887	1.5926	0.8250	0.8068	4.7596	4.5650

As shown in Table 1, en-RZT provides very accurate results for both thick and moderately thick plates. The percent errors between the en-RZT results and 3D-exact are not higher than 6% for thick and 3% for moderately thick plates.

Problem 2 - Cylindrical bending under sinusoidal load

To further assess the accuracy of en-RZT, especially in through-the-thickness distributions of local quantities, the problem of cylindrical bending is here considered. A three-layered symmetric angle-ply laminate (L2) is studied. The plate is of infinite length in the x_2 directions and uniformly supported along the edges. Thus in the equilibrium equations (31) and in the constitutive-plate relations (29) the derivatives with respect to x_2 are neglected. The plate is loaded by a sinusoidal transverse load of intensity $\bar{p}_3(x_1) = \bar{p}_0 \sin(\pi x_1 / a_1)$. The trigonometric expansions that satisfy the reduced equilibrium equations and consistent boundary conditions read

$$u_3 = U_3 \sin(\pi x_1 / a_1);$$
$$(u_1, u_2, \theta_1, \theta_2, \psi_1, \psi_2) = (U_1, U_2, \Theta_1, \Theta_2, \Psi_1, \Psi_2)\cos(\pi x_1 / a_1)$$

The three-dimensional elasticity solution has been obtained using the procedures developed by Pagano [16] for laminated plates in cylindrical bending. The FSDT solution here implemented uses only shear correction factor $k_1^2 = k_2^2 = 5/6$. The results for transverse shear stress distributions computed using FSDT, linear zigzag theory [5] (ZZT) and en-RZT are evaluated by integrating the 3D local equilibrium equations.

Figure 2 shows the through-the-thickness distributions of in-plane and transverse displacements and stresses of thick (a_1/h=4) angle-ply laminate (L2). The total transverse load is equally divided into two transverse loads applied on top and bottom external surfaces in the three-dimensional solution.

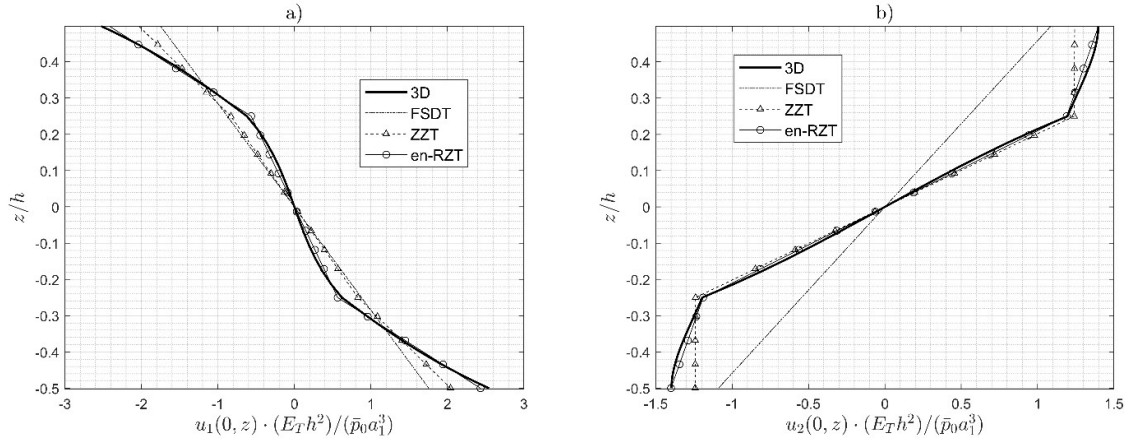

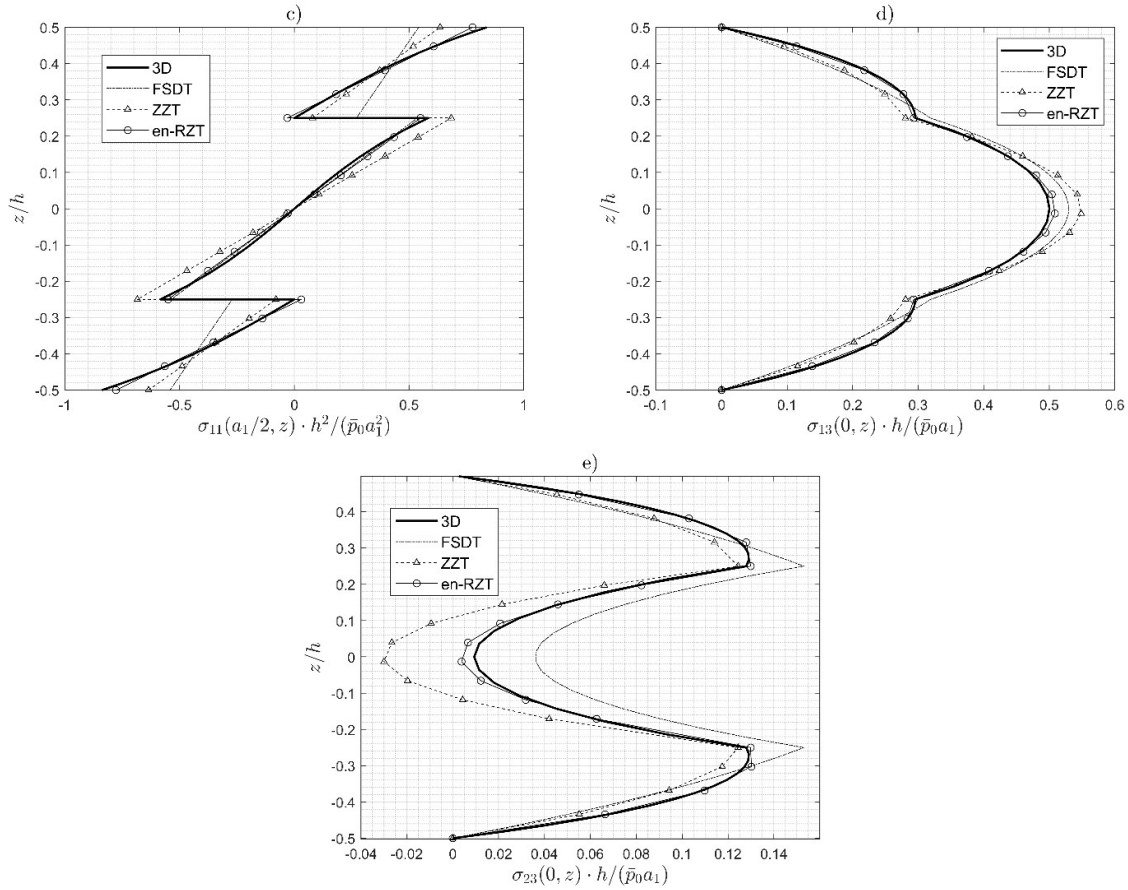

Figure 2 – Cylindrical bending of symmetric angle-ply laminate (L2), under sinusoidal transverse pressure ($a_1/h=4$). In figures 2d) and 2e), the values are computed using the integration of local equilibrium equations.

From Figure 2, the transverse displacement obtained using en-RZT is the only one close to the exact three-dimensional solution. Moreover, the in-plane displacement distributions obtained using en-RZT are in good agreement with the 3D Pagano's solution, the other theories being less accurate. It is clear from Figure 2 that FSDT is unable to predict the correct distributions of in-plane displacements and stresses. Furthermore, the enhanced method to obtain the zigzag functions of RZT allows predicting with more accuracy the local quantities compared to the ZZT.

4. Conclusions

An enhancement of Refined Zigzag Theory (en-RZT) is presented to study multilayered anisotropic composite plates. The enhanced local displacement field with a new set of zigzag functions allows introducing the coupling effect between the two in-plane displacements. Maintaining the same seven kinematic unknowns of standard RZT, the same partial continuity of the transverse shear stresses at the interfaces has been used to formulate this new set of functions. The resulting enhanced zigzag functions have the same property as those obtained in standard RZT, i.e. null value at the top and bottom plate surfaces. It has also been shown that this procedure is a generalisation of the zigzag functions used in

standard RZT. When symmetric/unsymmetric cross-ply multilayered plates are considered, the resulting enhanced zigzag functions are exactly the same as standard RZT. Moreover, this enhancement allows considering the *a-priori* neglected coupling effect in the partially transverse shear stress continuity formulated in standard RZT.

The investigated static problems show the improvements that the new functions have been introduced in RZT. Firstly, the possibility to study symmetric and anti-symmetric angle-ply multilayered plates, in which the same absolute value for the lamination angle is used for all layers. In fact, using standard RZT, it is not possible to compute a solution without changing the lamination angle for these kinds of plates. From the presented results, en-RZT is accurate enough to predict the maximum transverse displacement if compared with three-dimensional results. Moreover, the through-the-thickness quantities, such as in-plane displacements and stresses distributions, are closer to the exact three-dimensional solution than the other investigated theories.

Furthermore, en-RZT has the same computational advantage as standard RZT since it requires only C^0 continuity, while the TSDT requires C^1 continuity and fails in predicting the transverse shear stress at the clamped edge. In this sense, en-RZT does not fail in this drawback, and it has significant advantages in studying anisotropic multilayered structures. Moreover, the en-RZT still not require any shear correction factor.

In conclusion, this work shows the superior capability of the en-RZT to predict both global and local quantities accurately for anisotropic multilayered plates, specifically angle-ply lamination, for which the standard RZT fails. It is concluded that en-RZT could be used to study a wide range of generally laminated structures without increasing the model complexity. Finally, a further generalisation of RZT can be achieved by improving the local/global displacement fields increasing the accuracy to consider the nonlinear thickness-wise distributions of the three-dimensional solutions.

References

[1] Abrate, S., and Di Sciuva, M., 2017, "Equivalent Single Layer Theories for Composite and Sandwich Structures: A Review," Compos. Struct., **179**, pp. 482–494.

[2] Abrate, S., and Di Sciuva, M., 2018, "Multilayer Models for Composite and Sandwich Structures," *Comprehensive Composite Materials II*, P.W.R. Beaumont, and C.H. Zweben, eds., Elsevier, pp. 399–425.

[3] Whitney, J. M., 1969, "The Effect of Transverse Shear Deformation on the Bending of Laminated Plates," J. Compos. Mater., **3**(3), pp. 534–547.

[4] Murakami, H., 1986, "Laminated Composite Plate Theory With Improved In-Plane Responses," J. Appl. Mech., **53**(3), pp. 661–666.

[5] Di Sciuva, M., 1985, "Development of an Anisotropic, Multilayered, Shear-Deformable Rectangular Plate Element," Comput. Struct., **21**(4), pp. 789–796.

[6] Cho, M., and Parmerter, R. R., 1992, "An Efficient Higher-Order Plate Theory for Laminated Composites," Compos. Struct., **20**(2), pp. 113–123.

[7] Loredo, A., and Castel, A., 2014, "Two Multilayered Plate Models with Transverse Shear Warping Functions Issued from Three Dimensional Elasticity Equations," Compos. Struct., **117**, pp. 382–395.

[8] Loredo, A., D'Ottavio, M., Vidal, P., and Polit, O., 2019, "A Family of Higher-Order Single Layer Plate Models Meeting C_z^0-Requirements for Arbitrary Laminates," Compos. Struct., **225**, p. 14.

[9] Tessler, A., Di Sciuva, M., and Gherlone, M., 2009, "Refined Zigzag Theory for Laminated Composite and Sandwich Plates," NASATP-2009-215561, pp. 1–53.

[10] Tessler, A., Di Sciuva, M., and Gherlone, M., 2011, "A Homogeneous Limit Methodology and Refinements of Computationally Efficient Zigzag Theory for Homogeneous, Laminated Composite, and Sandwich Plates," Numer. Methods Partial Differ. Equ., **27**(1), pp. 208–229.

[11] Gherlone, M., 2013, "On the Use of Zigzag Functions in Equivalent Single Layer Theories for Laminated Composite and Sandwich Beams: A Comparative Study and Some Observations on External Weak Layers," J. Appl. Mech., **80**(6), pp. 1–19.

[12] Iurlaro, L., Gherlone, M., and Di Sciuva, M., 2015, "The (3,2)-Mixed Refined Zigzag Theory for Generally Laminated Beams: Theoretical Development and C^0 Finite Element Formulation," Int. J. Solids Struct., **73–74**, pp. 1–19.

[13] Kreja, I., and Sabik, A., 2019, "Equivalent Single-Layer Models in Deformation Analysis of Laminated Multilayered Plates," Acta Mech., **230**(8), pp. 2827–2851.

[14] Di Sciuva, M., 1992, "Multilayered Anisotropic Plate Models with Continuous Interlaminar Stresses," Compos. Struct., **22**(3), pp. 149–167.

[15] Savoia, M., and Reddy, J. N., 1992, "A Variational Approach to Three-Dimensional Elasticity Solutions of Laminated Composite Plates," J. Appl. Mech., **59**(2S), pp. S166–S175.

[16] Pagano, N. J., 1970, "Influence of Shear Coupling in Cylindrical Bending of Anisotropic Laminates," J. Compos. Mater., **4**(3), pp. 330–343.

345 **Table captions**

Table 1	Non-dimensional maximum deflections $\left(100u_3 \, E_T h^3 \big/ \bar{p}_0 a_1^4\right)$ of simply supported two-layered angle-ply plates (L1) under bi-sinusoidal transverse pressure

346

347

348 **Figure captions**

Figure 1	Zigzag functions for standard and enhanced RZT, anti-symmetric angle-ply (L1).
Figure 2	Cylindrical bending of symmetric angle-ply laminate (L2), under sinusoidal transverse pressure ($a_1/h=4$). In figures 2d) and 2e), the values are computed using the integration of local equilibrium equations.

349